THE JOURNAL OF PHYSICAL CHEMISTRY B

Article

Unfolding Thermodynamics of Intramolecular G-Quadruplexes: Base Sequence Contributions of the Loops

Chris M. Olsen, Hui-Ting Lee, and Luis A. Marky

J. Phys. Chem. B, **2009**, 113 (9), 2587-2595• DOI: 10.1021/jp806853n • Publication Date (Web): 14 November 2008

Unfolding Thermodynamics of Intramolecular G-Quadruplexes: Base Sequence Contributions of the Loops†

Chris M. Olsen,‡ Hui-Ting Lee,‡ and Luis A. Marky*,‡,§,||

Department of Pharmaceutical Sciences, Department of Biochemistry and Molecular Biology, and Eppley Institute for Cancer Research, University of Nebraska Medical Center, Omaha, Nebraska 68198-6025

Received: July 31, 2008; Revised Manuscript Received: September 24, 2008

G-quadruplexes are a highly studied DNA motif with a potential role in a variety of cellular processes and more recently are considered novel targets for drug therapy in aging and anticancer research. In this work, we have investigated the thermodynamic contributions of the loops on the stable formation of G-quadruplexes. Specifically, we use a combination of UV, circular dichroism (CD) and fluorescence spectroscopies, and differential scanning calorimetry (DSC) to determine thermodynamic profiles, including the differential binding of ions and water, for the unfolding of the thrombin aptamer: d(GGT_2GG*TGT*GGT_2GG) that is referred to as *G*2. The sequences in italics, *TGT* and T_2, are known to form loops. Other sequences examined contained base substitutions in the *TGT* loop (TAT, TCT, TTT, TAPT, and UUU), in the T_2 loops (T_4, U_2), or in both loops (UGU and U_2, UUU and U_2). The CD spectra of all molecules show a positive band centered at 292 nm, which corresponds to the "chair" conformation. The UV and DSC melting curves of each G-quadruplex show monophasic transitions with transition temperatures (T_Ms) that remained constant with increasing strand concentration, confirming their intramolecular formation. These G-quadruplexes unfold with T_Ms in the range from 43.2 to 56.5 °C and endothermic enthalpies from 22.9 to 37.2 kcal/mol. Subtracting the contribution of a G-quartet stack from each experimental profile indicated that the presence of the loops stabilize each G-quadruplex by favorable enthalpy contributions, larger differential binding of K^+ ions (0.1−0.6 mol K^+/mol), and a variable uptake/release of water molecules (−6 to 8 mol H_2O/mol). The thermodynamic contributions for these specific base substitutions are discussed in terms of loop stacking (base−base stacking within the loops) and their hydration effects.

Introduction

A tremendous amount of interest has been generated for the role of telomeres as a stabilizing entity maintaining the integrity of chromosomes.[1−5] Telomeres allow for the correct replication of eukaryotic chromosomes.[6] Telomeres are comprised of specific base sequences (usually G and T repeats of 12−16 bases) that in humans overhang on the 3′-end by 100−150 nucleotides; however, their possible formation of G-quadruplexes still remains under investigation.[7−9] A special RNA-dependent DNA polymerase enzyme called telomerase adds the repeating G-rich sequences to the 3′-end,[7] allowing for full replication of the other strand, preventing loss of important chromosomal information. Other potential roles of these G-quadruplexes include chromosomal alignment during recombination, DNA replication, self-recognition, and regulation of gene transcription.[10] Some DNA aptamers also form G-quadruplexes, examples include the thrombin-binding aptamer that inhibits thrombin-catalyzed fibrin clot formation[11,12] and the HIV-binding aptamer, T30695.[13] The *NHE-III* sequence, part of the promoter sequence of the c-MYC oncogene, that controls 80−90% of c-MYC transcription, also forms a G-quadruplex.[14−20] More recently, G-quadruplexes and telomerase have been proposed as ideal targets in the development of new anticancer therapies.[2]

G-quadruplexes are made up of guanine bases in DNA and RNA that associate via Hoogsteen hydrogen bonds to form planar G-quartets.[21] Guanine rich sequences can then form inter- or intramolecular G-quadruplexes. These G-quartets form a platform connected by intermediate sequences of several bases (loops). Loops play a key role in the overall folding and stability of G-quadruplexes;[8,9,22−24] therefore, the length and sequence of these loops can either stabilize or destabilize a G-quadruplex. This has been attributed to several types of molecular interactions, such as hydrogen bonding, base−base stacking interaction within the loops, and the stacking of the loops onto the G-quartets.[25−27]

Since their discovery, G-quadruplexes have become a highly studied DNA motif, due to their unique structural features and multiple potential roles in vivo.[7,28−33] Several groups have studied the roles of loops on the formation of various G-quadruplexes, including the human telomere sequence $d(T_2AG_3)_4$,[27,34−36] the tetramolecular G-quadruplex from *Oxytricha nova* telomeric sequence $[d(T_4G_4)]_4$, the bimolecular $[d(G_4T_4G_4)]_2$ also from *Oxytricha nova*,[34,37,38] and the thrombin aptamer $d(G_2T_2G_2TGTG_2T_2G_2)$, that inhibits thrombin-catalyzed fibrin clot formation.[12,26,34,39−41] The focus of this investigation is the thrombin aptamer, named hereafter as "*G*2", which readily forms an intramolecular G-quadruplex with a single G-quartet stack, interconnected with two TT loops (bottom) and one TGT loop (top) in the "chair" conformation. The sequence of these loops is modified, by base substitutions,

† Part of the "J. Michael Schurr Special Section".

* To whom inquires should be addressed. Tel.: (402) 559-4628. Fax: (402) 559-9543. E-mail: lmarky@unmc.edu.

‡ Department of Pharmaceutical Sciences, College of Pharmacy, University of Nebraska Medical Center, 986025 Nebraska Medical Center, Omaha, NE 68198-6025.

§ Department of Biochemistry and Molecular Biology.

|| Eppley Institute for Cancer Research.

10.1021/jp806853n CCC: $40.75
Published on Web 11/14/2008

SCHEME 1: G-Quadruplex Sequences, Designations, and Cartoon of Putative Structures with the 5′-End Indicated by the Bold Dot (•)

d($G_2T_2G_2TGTG_2T_2G_2$), *G2*

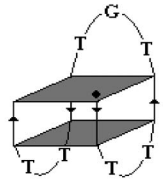

d($G_2U_2G_2TGTG_2U_2G_2$), *G2-U2U2*

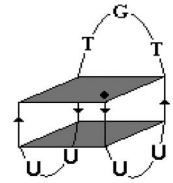

d($G_2T_2G_2TXTG_2T_2G_2$), *G2-TXT*

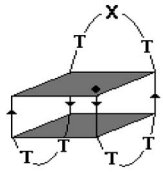

Where *X*= A, C, or T

d($G_2U_2G_2UGUG_2U_2G_2$), *G2-U*

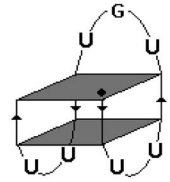

d($G_2T_4G_2TGTG_2T_4G_2$), *G2-T4T4*

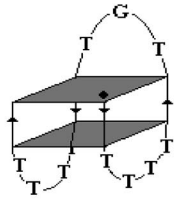

d($G_2T_2G_2UUUG_2T_2G_2$), *G2-UUU*

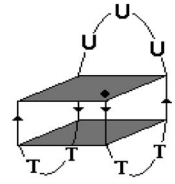

d($G_2T_2G_2TAPTG_2T_2G_2$), *G2-AP*

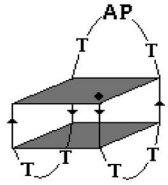

Where *AP* = 2- aminopurine

d($G_2U_2G_2UUUG_2U_2G_2$), *G2-UUU-U2U2*

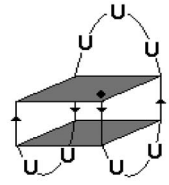

to determine their energetic, ion, and water binding contributions, using a combination of temperature-dependent UV and circular dichroism spectroscopies and differential scanning calorimetric techniques.

We report complete thermodynamic profiles for the temperature-unfolding of *G*2 with modified loop sequences (Scheme 1). The comparison of these profiles with those of *G*2 allows us to asses the relative contributions of the base modifications in the loops.

Experimental Details

Materials. The oligonucleotides (ODNs, and their designations), Scheme 1 d($G_2T_2G_2TGTG_2T_2G_2$), *G2*; d($G_2T_2G_2TXTG_2T_2G_2$), *G2-TXT*, where *X* = A, T, or C; d($G_2T_4G_2TGTG_2T_4G_2$), *G2-T4T4*; d($G_2T_2G_2TAPTG_2T_2G_2$), *G2-AP*, where AP = 2-amino purine; d($G_2U_2G_2TGTG_2U_2G_2$), *G2-U2U2*; d($G_2U_2G_2UGUG_2U_2G_2$), *G2-U*; d($G_2T_2G_2UUUG_2T_2G_2$), *G2-UUU*; and d($G_2U_2G_2UUUG_2U_2G_2$), *G2-UUU-U2U2*; were synthesized by the Core Synthetic Facility of the Eppley Research Institute at UNMC, HPLC purified, and desalted by column chromatography using G-10 Sephadex exclusion chromatography. The concentration of the oligomer solutions was determined at 260 nm and 80 °C using a Perkin-Elmer Lambda-10 spectrophotometer and the following molar extinction coefficients, in inverse micomolar centimeters: 146 (*G*2), 147 (*G2-TAT*), 141 (*G2-TTT*), 144 (*G2-TCT*), 186 (*G2-T4T*4), 148 (*G2-AP*), 148 (*G2-U2U*2), 156 (*G2-U*), 149 (*G2-UUU*), and 158 (*G2-UUU-U2U*2). These values were obtained by extrapolation of the tabulated values for dimers and monomeric bases at 25 °C[42,43] to higher temperatures using procedures reported earlier.[44] Inorganic salts from Sigma were reagent grade and used without further purification. All measurements were made in buffer solutions containing 10 mM Cs-HEPES at pH = 7.5, adjusted to the desired salt concentration with KCl or CsCl. Oligonucleotide solutions were prepared by dissolving the dry and desalted ODN in buffer, the Cs^+/K^+ ion exchange was done

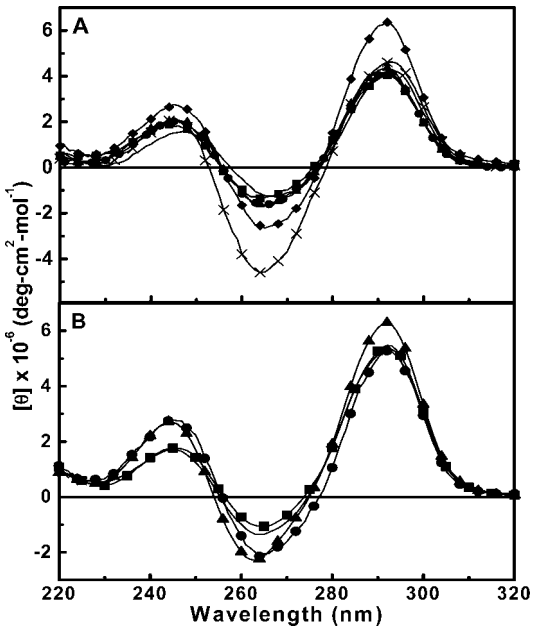

Figure 1. Typical CD spectra of G-quadruplexes in 10 mM Cs-HEPES, 100 mM KCl at pH 7.5, and at a total strand concentration of ~6 μM in strands: (A) *G2* and loop modified *G2* without dU substitutions, *G2* (line), *G2-TAT* (■), *G2-TTT* (•), *G2-TCT* (▲), *G2-T4T4* (×), *G2-AP* (◆); (B) *G2* loop modified with dU substitutions, *G2-U* (line), *G2-UUU* (•), *G2-U2U2* (■), *G2-UUU-U2U2* (▲).

initially by heating the ODN solution to 100 °C for 5 min and cooled to room temperature over 25 min.

Circular Dichroism Spectroscopy (CD). The conformation of each G-quadruplex in the presence of K^+-ions was obtained using an Aviv Circular Dichroism Model 202SF spectrometer (Lakewood, NJ) equipped with a peltier temperature control system. Spectra were obtained from 340 to 220 nm in 1 nm increments and the reported spectra correspond to the average of at least two wavelength scans. The conformation of the complex was determined by inspection of the CD spectra at low temperatures. CD melting curves were performed by following the change in ellipticity as a function of temperature at 262 or 292 nm. ODN solutions were heated at a rate of ~0.9 °C/min, using strain-free quartz cuvettes with a path length of 0.1 or 1.0 cm, resulting with the collection of 1−2 data points/°C. It should be pointed out that melting curves obtained at heating rates below 1 °C/min and, for short oligonucleotides, indicate reversible curves at equilibria. Analysis of the CD melting curves, using standard procedures,[44] yielded transition temperatures, T_Ms, which are the midpoint temperatures of the complex-coil transitions, and model dependent van't Hoff enthalpies, ΔH_{vH}.[44]

Temperature-Dependent UV and Fluorescence Spectroscopies. Absorbance versus temperature profiles were measured at 260 and/or 297 nm with a thermoelectrically controlled Aviv spectrophotometer Model 14DS UV−vis (Lakewood, NJ) or Perkin-Elmer Lambda-10 UV−vis spectrophotometer. The temperature was scanned from 10 to 100 °C at a heating rate of ~0.6 °C/min. Shape analysis of the melting curves yielded T_Ms and ΔH_{vH}s using standard procedures.[44,45] The transition molecularity for the unfolding of a particular complex was determined from the T_M dependence on strand concentration. The T_M of intramolecular complexes does not depend on strand concentration while the T_M of intermolecular complexes does depend on strand concentration.

The fluorescent emission spectra of the 2-aminopurine substituted G-quadruplex (*G2-AP*) were obtained at low and high temperatures on a thermoelectrically controlled Cary Eclipse fluorescence spectrophotometer (Varian, Walnut Creek, CA) to determine a suitable emission wavelength to use in the fluorescence melt. A fluorescent melting curve was obtained by monitoring the emission fluorescence changes at 380 nm from 2 to 100 °C, at a heating rate of ~0.6 °C/min, using an excitation wavelength of 320 and 5 nm slits.

Differential Scanning Calorimetry (DSC). The total heat required for the unfolding of each G-quadruplex was measured with a VP-DSC differential scanning calorimeter from Microcal (Northampton, MA). Standard thermodynamic profiles and T_Ms are obtained from DSC experiment using the following relationships: $\Delta H_{cal} = \int \Delta C_p(T)\, dT$; $\Delta S_{cal} = \int \Delta C_p(T)/T\, dT$; and the Gibbs equation, $\Delta G^\circ_{(20)} = \Delta H_{cal} - T\Delta S_{cal}$; where ΔC_p is the anomalous heat capacity of the ODN solution during the unfolding process, ΔH_{cal} is the unfolding enthalpy, and ΔS_{cal} is the entropy of unfolding. Both latter terms are temperature-dependent, i.e., the heat capacity difference between the initial and final states is nonzero. Alternatively, ΔG°_T can be calculated using the equation $\Delta G^\circ_T = \Delta H_{cal}(1 - T/T_M)$ which is implicitly correct for the unfolding of intramolecular complexes such as these G-quadruplexes. The ΔH_{vH} terms are also obtained from the DSC profiles using the temperatures at the half-width height of the experimental curve.[44] The $\Delta H_{vH}/\Delta H_{cal}$ ratio can tell us about the nature of the transition, for a two-state transition $\Delta H_{vH} = \Delta H_{cal}$, while for non-two-state, $\Delta H_{vH} \neq \Delta H_{cal}$.[44,45]

Determination of the Differential Binding of Counterions and Water. Additional UV melting curves, as a function of salt and osmolyte concentrations, were performed to determine the differential binding of counterions, Δn_{K^+}, and water molecules, Δn_W, between the quadruplex and coil states. The Δn_{K^+} and Δn_W linking numbers represent the uptake (or release) of counterions and water, respectively, for the helix-coil transition of each complex and are measured experimentally using the following relationships: $(\partial \ln K/\partial \ln(K^+)) = \Delta n_{K^+}$ and $(\partial \ln K/\partial \ln(a_W)) = \Delta n_W$. In each of these relationships, it is assumed a similar type of counterion, or water, binding to both helical and random coil states.[46] Application of the chain rule yields:

$$\Delta n_{K^+} = (\partial \ln K/\partial T_M)(\partial T_M/\partial \ln(K^+)) = 1.11[\Delta H_{cal}/RT_M^2](\partial T_M/\partial \ln[K^+]) \quad (1)$$

$$\Delta n_W = (\partial \ln K/\partial T_M)(\partial T_M/\partial \ln(a_W)) = [\Delta H_{cal}/RT_M^2](\partial T_M/\partial \ln a_W) \quad (2)$$

The terms in brackets of Eqs 1 and 2 are determined directly from DSC experiments while the ones in parentheses from UV melts. The latter correspond to the slopes of the plots of T_M as a function of the concentration of potassium and water activity respectively.[47] The value 1.11 in eq 1 is a constant which is used to convert activities into concentration terms. The activity of water is varied by using different concentrations of a cosolute, ethylene glycol, which does not interact with the ODN.[48] The osmolality of these solutions were obtained using a UIC vapor pressure osmometer Model 830, calibrated with standardized NaCl solutions, and then converted into activities using the following equation: $\ln a_W = -\text{Osm}/M_W$, where Osm is the solution of osmolality and M_W is the molality of pure water equal to 55.5 mol/kg of H_2O.

Results

CD Spectra and Conformational Analysis. The average solution conformation of a G-quadruplex can be obtained using

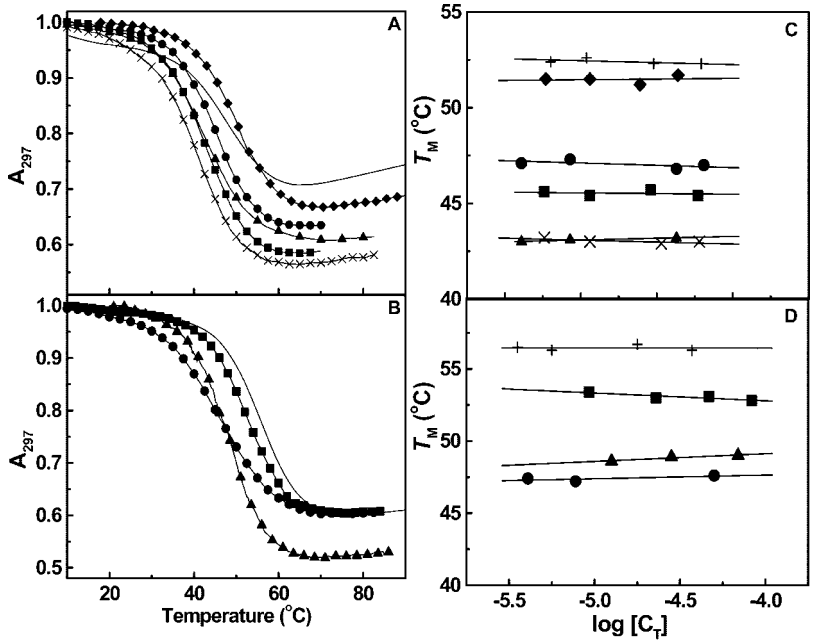

Figure 2. Typical UV-melting curves of G-quadruplexes in 10 mM Cs-HEPES, 100 mM KCl at pH 7.5, and at a total strand concentration of ~5 μM in strands: (A) *G*2 and loop modified *G*2 without dU substitutions, *G*2 (–), *G2-TAT* (■), *G2-TTT* (•), *G2-TCT* (▲), *G2-T4T4* (×), *G2-AP* (◆); (B) *G*2 loop modified with dU substitutions, *G2-U* (–), *G2-UUU* (•), *G2-U2U2* (■), *G2-UUU-U2U2* (▲). The T_M dependences on strand concentration for each G-quadruplex are shown in parts C and D. The symbols are as in A and B, respectively, and (+) for *G*2 and *G2-U*.

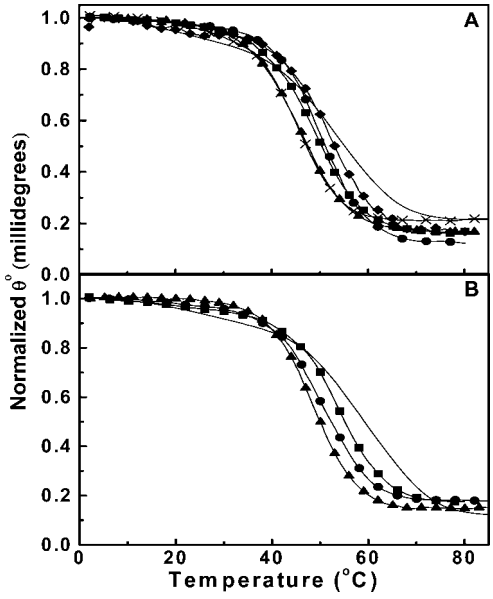

Figure 3. Typical CD melting curves of G-quadruplexes in 10 mM Cs-HEPES, 100 mM KCl at pH 7.5, and at a total strand concentration of ~6 μM in strands: (A) *G*2 and loop modified *G*2 without dU substitutions, *G*2 (line), *G2-TAT* (■), *G2-TTT* (•), *G2-TCT* (▲), *G2-T4T4* (×), *G2-AP* (◆); (B) *G*2 loop modified with dU substitutions, *G2-U* (line), *G2-UUU* (•), *G2-U2U2* (■), *G2-UUU-U2U2* (▲).

CD spectroscopy. CD spectra are taken at several temperatures to determine the preferred conformation of the cation−aptamer complex at lower temperatures and the random coil state at higher temperatures. All molecules folded quickly and were reproducible i.e., did not require the temperature treatment of other G-quadruplexes.[26]

Representative CD spectra of each molecule are shown in Figure 1A and B. The spectrum of *G*2 has a large positive band centered at 292 nm, a smaller negative band at 264 nm, and smaller positive band at 246 nm.[26,40,49,50] The spectral characteristics of the other molecules are similar to the spectrum of *G*2 with differences in the magnitudes of the bands. For instance, *G2-T4T4* has a larger negative band at 264 nm, due to larger thymine loops;[40] *G2-AP* has larger intensities at each of these three bands, which may be due to increase stacking interactions. This will be further studied in later sections. All molecules with dU residues showed an increase in the signal at 292 nm that may be due to the higher hydrophilicity of this residue; while the magnitude of the bands at 264 and 246 nm were comparable to those of the *G*2, *G2-TAT*, *G2-TCT*, and *G2-TTT* molecules. On the basis of the shape similarities of these spectra with the CD spectra of the bimolecular G-quadruplex with sequence $d(G_4T_4G_4)$,[41] we conclude that all molecules have an antiparallel arrangement of guanines at each face.[26,40,49,50] The alternating 5′ to 3′ directionality of the guanines indicates that these G-quadruplexes adopt the chair conformation.[23]

TABLE 1: Model-Dependent Unfolding Enthalpies (ΔH_{vH})[a]

	ΔH_{vH} (DSC)	ΔH_{vH} (CD)	ΔH_{vH} (UV)	avg ΔH_{vH}
*G*2	40	41	42	41
G2-TAT	37	42	38	39
G2-TCT	38	40	35	38
G2-TTT	39	44	43	42
G2-T4T4	39	40	39	39
G2-AP	43	46	50	46
G2-U2U2	44	47	48	46
G2-U	32	36	38	35
G2-UUU-U2U2	48	44	46	46
G2-UUU	41	39	31	37

[a] All experiments were performed in 10 mM Cs-Hepes buffer and 100 mM KCl, at pH 7.5. All values are in kilocalories per mole, and their experimental error is 15%.

UV and CD Unfolding of Complexes. Typical UV melting curves at 297 nm are shown in Figure 2A and B, this wavelength was chosen because of its larger absorbance difference between the low- and high-temperature UV spectra (data not shown). All curves are sigmoidal and show a hypochromic effect at 297 nm. The helix−coil transition of each G-quadruplex takes place in monophasic transitions. The observed hypochromicities for

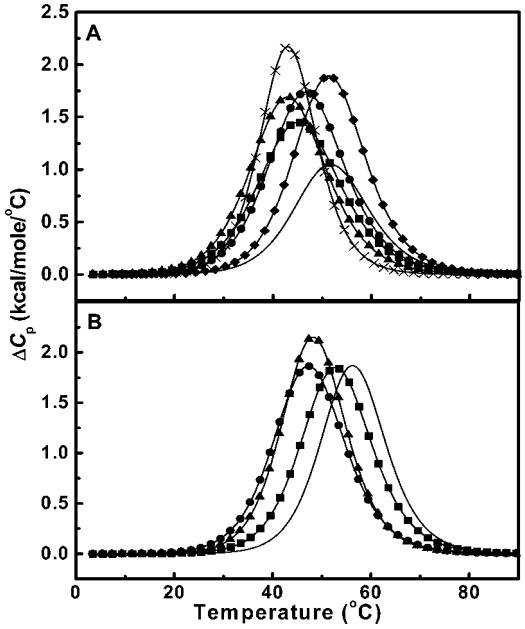

Figure 4. Typical DSC melting curves of G-quadruplexes in 10 mM Cs-HEPES, 100 mM KCl at pH 7.5, and at a total strand concentration of ~40−100 μM: (A) *G*2 and loop modified *G*2 without dU substitutions, *G*2 (line), *G*2-*TAT* (■), *G*2-*TTT* (•), *G*2-*TCT* (▲), *G*2-*T*4*T*4 (×), *G*2-*AP* (◆); (B) *G*2 loop modified with dU substitutions, *G*2-*U* (line), *G*2-*UUU* (•), *G*2-*U*2*U*2 (■), *G*2-*UUU*-*U*2*U*2 (▲).

these transitions ranged from 28% (*G*2) to 47% (*G*2-*UUU*-*U*2*U*2). The T_Ms follow the order: *G*2-*T*4*T*4 (43.0 °C) < *G*2-*TCT* < *G*2-*TAT* < *G*2-*TTT* < *G*2-*UUU* < *G*2-*UUU*-*U*2*U*2 < *G*2-*AP* < *G*2 < *G*2-*U*2*U*2 < *G*2-*U* (56.8 °C). These data indicate the extremely high stability of G-quadruplex structures in the presence of K^+. To check the molecularity of each complex, melting curves were obtained as a function of strand concentration and over a 10-fold range in strand concentration. The T_Ms for each molecule remained constant, indicating that all quadruplexes formed intramolecularly (Figure 2C).

CD melting curves were also performed at wavelengths with the largest difference in ellipticity: 292 nm for *G*2 and each of the loop modified aptamers (Figure 3). All CD melting curves showed monophasic transitions. The T_Ms of all molecules are in good agreement with those obtained from UV melts. Shape analysis of the UV and CD melting curves yielded ΔH_{vH} values ranging from −31 (*G*2-*UUU*) to −50 kcal/mol (*G*2-*AP*), see Table 1, which will be discussed in the following section.

DSC Unfolding. Typical DSC unfolding curves for each G-quadruplex are shown in Figure 4. The unfolding of each molecule undergoes highly reproducible monophasic transitions. Furthermore, the initial and final states of each transition have similar heat capacity values, which indicate that their unfolding is accompanied by negligible heat capacity effects. The T_Ms obtained from the calorimetric melts (Table 2) are similar to those obtained from UV and CD melts, in spite of different strand concentrations, and consistent with their intramolecular formation.

The complete thermodynamic profiles for the folding of each quadruplex at 20 °C are shown in Table 2. The favorable $\Delta G°$ for the formation of each quadruplex ranges from −2.3 kcal/mol (*G*2) to −3.6 kcal/mol (*G*2-*U*, *G*2-*U*2*U*2, and *G*2-*AP*) and results from the characteristic compensation of a favorable enthalpy term with an unfavorable entropy contribution. The favorable enthalpy terms, ΔH_{cal} from −22.9 kcal/mol (*G*2) to −37.2 kcal/mol (*G*2-*UUU*-*U*2*U*2), are due primarily to the stacking of two G-quartets and additional contributions from base−base stacking within the loops and/or stacking of the loops onto the G-quadruplex. The immobilization of electrostricted water, if any, and the putative removal of structural water may also contribute with exothermic heats. The unfavorable entropy contribution is mainly due to the ordering of a random coil into an intramolecular quadruplex and uptake of ions and water molecules.

The nature of each transition was analyzed by simple inspection of the $\Delta H_{vH}/\Delta H_{cal}$ ratio. The average ΔH_{vH} values of the UV, CD, and DSC experiments are shown in Table 1; most are higher than the calorimetric enthalpies. We obtained $\Delta H_{vH}/\Delta H_{cal}$ ratios of 1.15 ± 0.20 for the majority of the G-quadruplexes, indicating that these molecules unfold in a two-state fashion, i.e. no intermediate states are present. The exceptions were *G*2 and *G*2-*AP* that have $\Delta H_{vH}/\Delta H_{cal}$ ratios in excess of one, 1.7 ± 0.3 and 1.3 ± 0.3, respectively, which may be due to the presence of end-to-end aggregates,[41] perhaps due to the aggregating tendency of the guanine like residues in the TGT and TAPT loops of these quadruplexes.

Differential Binding of K^+. UV melting curves as a function of the concentration of K^+ were performed in the 10−250 mM KCl range (data not shown). T_M dependences on salt are shown in Figure 5A and B, and the Δn_{K^+} terms were calculated with eq 1 and are summarized in Table 3. For the formation of each quadruplex, negative Δn_{K^+} values are obtained ranging from −0.4 mol K^+/mol quadruplex (*G*2) to −0.9 mol K^+/mol quadruplex (*G*2-*T*4*T*4). This indicates that the folding of a quadruplex is accompanied by an uptake of K^+, i.e. salt is stabilizing the quadruplex structure. This is consistent with the quadruplex state having the higher charge density parameter. These Δn_{K^+} values correspond to an average of 0.094−0.225 mol K^+/mol of phosphate, if only the phosphates within the G-quartets are considered. This value is larger than the average value of 0.077 mol Na^+/mol phosphate, obtained from the formation of nine hairpins containing 4 GC base pairs in the stem and considering only the stem phosphates.[51,52] These larger values suggest that G-quadruplexes bind K^+ more effectively, which may be due to their higher charge density parameter, in agreement with the additional K^+ ion needed to stabilize the formation of a G-quartet stack.[23,24] Furthermore, the larger Δn_{K^+} value of *G*2-*T*4*T*4 may be due to the increased number of bases in the thymine loops, which are folded in a compact way and thus increasing the charge density parameter of this G-quadruplex.

Differential Binding of Water. UV melting curves as a function of osmolyte (ethylene glycol) concentration were performed in the 0.5−3 M range (data not shown). Increasing the concentration of ethylene glycol (decreasing water activity) had a small effect on the T_M (1−4 °C). The T_M dependences on the activity of water are shown in Figure 5C and D. The differential binding of water between the G-quadruplex and random coil states were calculated with eq 2. We obtained positive Δn_W values for the formation of each quadruplex (Table 3), indicating that the folding of a G-quadruplex is accompanied by a release of water molecules,[26,53] i.e., the random coil state is the more hydrated stated in these molecules. Specifically, these Δn_W terms ranged from 7 mol H_2O/mol quadruplex (*G*2-*T*4*T*4) to 21 mol H_2O/mol quadruplex (*G*2-*TTT*) for the non T → U substituted G-quadruplexes and from 7 mol H_2O/mol quadruplex (*G*2-*U*2*U*2, *G*2-*UUU*-*U*2*U*2) to 15 mol H_2O/mol (*G*2-*UUU*) for the T → U substituted G-quadruplexes. To explain these ranges of values, we invoke several hydration and compensating contributions in the folding of a quadruplex:[26,41] release of

TABLE 2: Thermodynamic Folding Profiles of G-Quadruplexes[a]

oligomer	T_M (°C)	ΔH_{cal} (kcal/mol)	$\Delta G^\circ_{(20)}$ (kcal/mol)	$T\Delta S_{cal}$ (kcal/mol)
G2	52.4	−22.9	−2.3	−20.6
G2-TAT	45.5	−32.3	−2.6	−29.7
G2-TCT	43.3	−34.6	−2.5	−32.1
G2-TTT	47.0	−35.7	−3.0	−32.7
G2-AP	51.6	−36.6	−3.6	−33.0
G2-T4T4	43.2	−33.5	−2.5	−31.0
G2-U2U2	53.1	−35.3	−3.6	−31.7
G2-U	56.5	−33.0	−3.6	−29.4
G2-UUU-U2U2	48.5	−37.2	−3.3	−33.9
G2-UUU	47.6	−35.9	−3.1	−32.8

[a] All experiments were done in 10 mM Cs-Hepes buffer and 100 mM KCl at pH 7.5. The experimental errors are as follows: T_M (±0.5 °C), ΔH_{cal} (±5%), $\Delta G^\circ_{(20)}$ (±7%), and $T\Delta S$ (±5%).

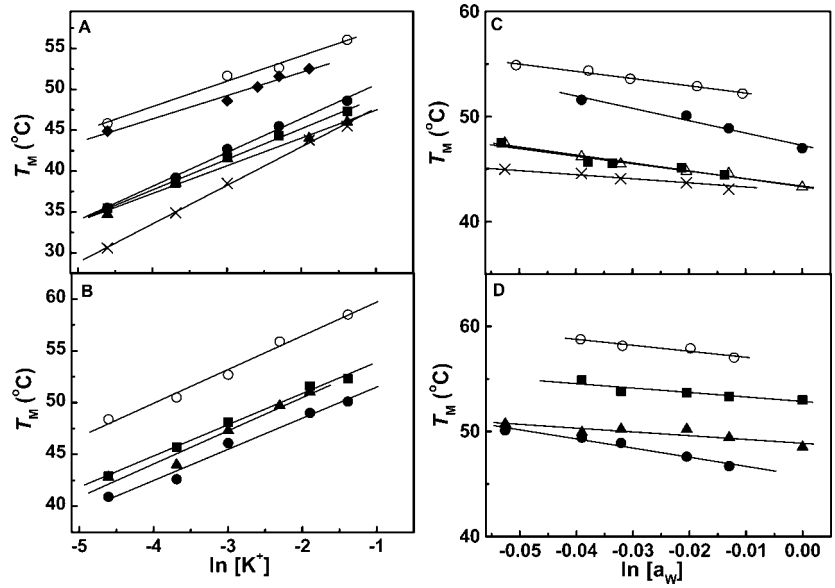

Figure 5. T_M dependence on [K^+] of *G2* and loop modified *G2* without dU substitutions (A) *G2* (○), *G2-TAT* (■), *G2-TTT* (•), *G2-TCT* (▲), *G2-T4T4* (×), *G2-AP* (◆) and with dU substitutions (B) *G2-U* (○), *G2-UUU* (•), *G2-U2U2* (■), *G2-UUU-U2U2* (▲). T_M dependence on a_W of *G2* and loop modified *G2* without dU substitutions (C) and with dU substitutions (D). The symbols are as in A and B, respectively.

TABLE 3: Differential Thermodynamic Binding of Ions (Δn_{K^+}) and Water (Δn_W)[a]

oligomer	$RT_M^2/\Delta H_{cal}$ (K)	$\partial T_M/\partial$ ln[K^+] (K)	Δn_{K^+} (per mol)	$\partial T_M/\partial$ ln a_W (K)	Δn_W (per mol)
G2	−9.20	3.10	−0.4	−68.7	8
G2-TAT	−6.25	3.75	−0.7	−71.3	11
G2-TCT	−5.75	3.40	−0.7	−75.6	13
G2-TTT	−5.70	4.14	−0.7	−118	21
G2-AP	−5.73	2.84	−0.6	nd	nd
G2-T4T4	−5.94	4.72	−0.9	−38.7	7
G2-U2U2	−5.99	3.02	−0.6	−42.7	7
G2-U	−6.54	3.26	−0.6	−57.0	9
G2-UUU-U2U2	−5.53	3.21	−0.6	−36.0	7
G2-UUU	−5.69	3.01	−0.6	−87.0	15

[a] The salt dependences were done in 10 mM Cs-HEPES buffer at pH 7.5 and adjusted to the desired salt concentration with KCl, while the dependences on the activity of water were determined in the same buffer with the inclusion of 0.1 M KCl and adjusted to the desired osmolyte concentration with ethylene glycol. The experimental errors are as follows: Δn_{K^+} (±7%) and Δn_W (±10%).

structural water from the random coil state; uptake of electrostricted water by the quadruplex, due to its higher charge density parameter; and the release of electrostricted water from K^+ upon binding to the G-quadruplex core.

Discussion

Thermodynamic Profiles for the Formation of a G-quadruplex. We have used a combination of temperature-dependent spectroscopies and calorimetric techniques to measure complete thermodynamic profiles for the unfolding of several G-quadruplexes. The overall results are shown in Tables 2 and 3 for the folding of each G-quadruplex. In general, the favorable folding of a particular G-quadruplex (negative ΔG°) results from the characteristic compensation of a favorable enthalpy and unfavorable entropy contributions, uptake of K^+ ions and a net release of water molecules. The main parameters determining the favorable $\Delta G^\circ_{(T)}$ terms are the enthalpy and the T_M; therefore, the higher stability (more negative $\Delta G^\circ_{(T)}$) of the base-substituted G-quadruplexes (relative to *G2*) is due to more favorable enthalpy changes since their T_Ms are lowered. We speculate that

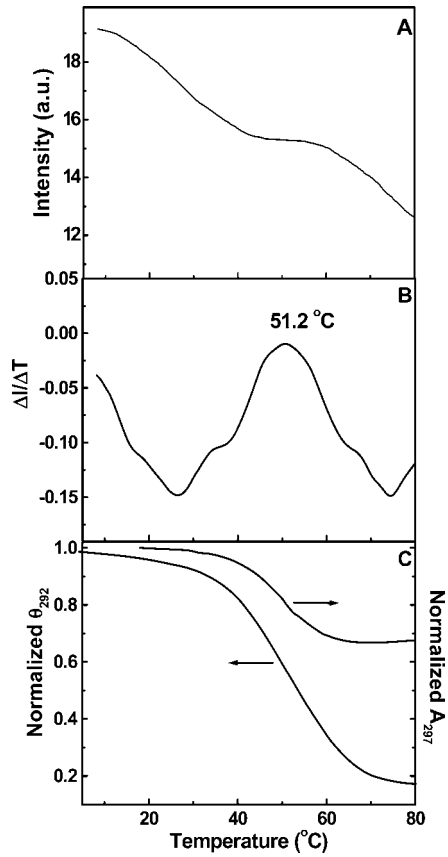

Figure 6. Typical fluorescent melting curve of *G2-AP* in 10 mM Cs-HEPES, 100 mM KCl at pH 7.5, and at a total strand concentration of ~4 μM (A) and its corresponding derivative curve (B). Excitation and emission wavelengths were set at 320 and 380 nm, respectively, using 5 nm slits. The UV and CD melting curves of the same solution are shown in part C.

their lower T_Ms are due to entropy effects, corresponding to the interaction of the G-quadruplex with ions and water.

Thermodynamic Contributions of the Loops. We used the reported thermodynamic profile for the formation of a single G-quartet stack[26] to estimate the thermodynamic contributions of the loops of each G-quadruplex. The thermodynamic contributions of a single G-quartet stack ($\Delta G^\circ_{20} = -2.2$ kcal/mol, $\Delta H_{cal} = -14.6$ kcal/mol, $T\Delta S_{cal} = -12.4$ kcal/mol, $\Delta n_{K+} = -0.3$ mol K^+/mol, and $\Delta n_W = 13$ mol H_2O/mol) were subtracted from the experimental thermodynamic profile of each G-quadruplex (Table 2 and 3) to yield the profiles shown in Table 4. The differential $\Delta G°$ terms is −0.1 kcal/mol (*G2*) and ranged from −0.3 kcal/mol (*G2-TCT*) to −1.4 kcal/mol (*G2-AP*) for non-dU substituted *G2*; and from −0.9 kcal/mol (*G2-UUU*) to −1.4 kcal/mol (*G2-U2U2* and *G2-U*) for dU substituted *G2*. This exercise shows that the incorporation of loops stabilizes the G-quadruplex structure due to favorable enthalpic contributions. The differential ΔH_{cal} term is −8.3 kcal/mol (*G2*) and ranged from −17.7 kcal/mol (*G2-TAT*) to −22.0 kcal/mol (*G2-AP*) for non-dU substituted *G2*; and from −18.4 kcal/mol (*G2-U*) to −22.6 kcal/mol (*G2-UUU-U2U2*) for dU substituted *G2*. The loops of all G-quadruplexes contribute with an additional uptake of ions of 0.1 mol K^+/mol (G2); 0.4 mol K+/mol (non-dU substituted *G2*), the exception is *G2-T4T4* (0.6 mol K^+/mol) due to the additional 4 thymines; and 0.3 mol K^+/mol (dU substituted *G2*). In terms of the differential binding of water, the loops of *G2* yielded an uptake of 5 mol H_2O/mol, the non-dU substituted loops showed values ranging from −6 mol H_2O/mol (*G2-T4T4*) to 8 mol H_2O/mol (*G2-TTT*), while the dU substituted loops showed values ranging from −6 mol H_2O/mol (*G2-UUU-U2U2*) to 2 mol H_2O/mol (*G2-UUU*). These hydration differences are associated with the overall compactness of the loops, if they are stacked onto the G-quartets and/or base−base stacking within the loops, and the contributions due to the presence of the thymine methyl groups that immobilize structural water. The main observation is that the incorporation of any type of base substitutions in the loops of *G2* results in more stable G-quadruplexes, due to more exothermic heat contributions (by −20 kcal/mol, uptake of counterions (by 0.35 mol K^+/mol) and a variable uptake/release of water molecules.

The favorable enthalpy contribution of the loops indicates that base-stacking occurs within these loops, and that these loops may stack onto the G-quartets. This is in agreement with the NMR solution structure of *G2*[23,24] that indicated the guanine of the TGT loop is stacked on top of the G-quartets with the thymine methyl groups pointing out toward the solvent. On the other hand, the methyl groups of the two other loop thymines are pointed toward each other to perhaps minimize their exposure to the solvent.

To determine if the loops are stacked onto the G-quadruplex, a fluorescent melt of *G2-AP* was done (Figure 6). This quadruplex contained a 2-aminopurine base, a fluorescent analog of guanine and adenine, instead of a guanine in the TGT loop. As the temperature is increased, there is a gradual decrease in the fluorescence intensity up to ~40 °C, followed by a leveling off of this intensity i.e. a broad monophasic transition with a T_M of –51 °C is obtained (Figure 6B), and a further decrease in

TABLE 4: Thermodynamic Contributions of the Base-Substituted Loops[a]

oligomer	$\Delta\Delta H_{cal}$ (kcal/mol)	$\Delta(T\Delta S_{cal})$ (kcal/mol)	$\Delta\Delta G^\circ_{20}$ (kcal/mol)	$\Delta\Delta n_{K^+}$ (per mol)	$\Delta\Delta n_W$ (per mol)
G2	−8.3	−8.2	−0.1	−0.1	−5
		substitutions of G in the TGT loop			
G2-TAT	−17.7	−17.3	−0.4	−0.4	−2
G2-TCT	−20.0	−19.7	−0.3	−0.4	0
G2-TTT	−21.1	−20.3	−0.8	−0.4	+8
G2-AP	−22.0	−20.6	−1.4	−0.3	nd
G2-T4T4	−18.9	−18.6	−0.3	−0.6	−6
		base substitutions of the TGT and TT loops			
G2-U2U2	−20.7	−19.3	−1.4	−0.3	−6
G2-UUU-U2U2	−22.6	−21.5	−1.4	−0.3	−6
G2-U	−18.4	−17.0	−1.4	−0.3	−5
G2-UUU	−21.3	−20.4	−0.9	−0.3	+2

[a] All values were obtained by subtracting the G-quartet stacking contributions[26] from the experimental thermodynamic profile of each G-quadruplex. The experimental errors are as follows: $\Delta\Delta H_{cal}$ (±7%), $\Delta\Delta G^\circ_{20}$ (±9%), $\Delta(T\Delta S)$ (±7%), $\Delta\Delta n_{K^+}$ (±9%), and $\Delta\Delta n_W$ (±14%).

the intensity as the temperature reaches 80 °C. These fluorescence changes clearly indicate the changes that AP is experiencing with temperature, including exposure of the AP base to solvent, and changes in the binding of ions and water by the loop. Furthermore, the UV and CD melting curves of *G2-AP* (Figure 6C) show monophasic transitions with T_Ms of 51 °C, which follow the unfolding of the entire G-quadruplex. Therefore, the comparison of these three types of melting curves indicate the transition of the fluorescence melting curve follows the unfolding of the entire G-quadruplex, and its small fluorescence changes correspond to base−base unstacking of the top loop. We estimated a ΔH_{vH} of 40 ± 4 kcal/mol for this transition which is much larger than the unfolding heat of the loops ($\Delta\Delta H_{cal}$ = 22.0 kcal/mol) and similar to the unfolding of the whole *G2-AP* quadruplex (ΔH_{cal} = 36.6 kcal/mol). This apparent discrepancies invoke interactions of the loops with ions and water molecules, which is reflected by the high sensitivity of the fluorescence melting curve. Furthermore, since ionic contributions contribute with negligible heats,[54,55] we speculate that these unfolding heats correspond to both unstacking of the loop bases and associated hydration effects resulting from a net exchange of electrostricted/structural water. We conclude that the inclusion of fluorescent bases in the loops of G-quadruplexes is a helpful way to study the molecular interactions and contributions of the loops.

To determine the thermodynamic contributions for specific base substitutions in the loops of *G2*, we compare thermodynamic profiles for pairs of molecules with the assumption that their random coil states are similar at high temperatures. The substitution of G for A, C, or T yielded more stable molecules, −0.2 kcal/mol (C) to −0.7 (T) kcal/mol, due to favorable exothermic heats of −9.4 kcal/mol (A) to −12.8 kcal/mol (T), similar uptake of ions (−0.3 mol K^+/mol) and variable water releases, 3 mol H_2O/mol (A) to 13 mol H_2O/mol (T). The overall effects suggest a rearrangement of the substituted loops: unstacking of the loop from the G-quartet and increased stacking interactions within the loop bases, yielding an increased ion binding and a higher release of water molecules. This is also consistent with the higher exothermic heat (by −13.7 kcal/mol) in the G → AP substitution. The increase in the number of thymines (from 2 to 4) in the T2 loops of *G2* also yielded slightly more stable quadruplex (by −0.2 kcal/mol), due to a more favorable heat of −10.6 kcal/mol (T), larger uptake of ions (−0.5 mol K^+/mol), and a marginal water uptake of 1 mol H_2O/mol. This is explained in terms of increased stacking interactions within the thymines loops.

The substitution of the *T2* loops of *G2* with *U2* loops (*G2* → *G2-U2U2*) yielded a much more stable G-quadruplex (by −1.3 kcal/mol), due to a higher exothermic heat (−12.4 kcal/mol), marginal uptake of ions (−0.2 mol K^+/mol) and water molecules (1 mol H_2O/mol), while the additional substitution of the thymines in the TGT loop (*G2-U2U2* → *G2-U*) resulted in a release of 2 mol H_2O/mol and similar thermodynamic contributions. One possible explanation for the latter hydration effect is the removal of structural water, associated with the loss of two methyl groups. The further substitution of the guanine in the UGU loop with uridine (*G2-U* → *G2-UUU-U2U2*) yielded a slightly less stable G-quadruplex (by −0.3 kcal/mol), exothermic heat of −4.2 kcal/mol, and uptake of 2 mol H_2O/mol. This suggests that this heat may be associated with the unstacking of the guanine/loop and with the rearrangement of the solvent, yielding more hydrophilic molecules.

In the following Hess cycles we gradually incorporate methyl groups to the two types of loops. The substitution of the U2 loops of *G2-UUU-U2U2* with thymines (*G2-UUU-U2U2* → *G2-UUU*) yields a less stable G-quadruplex (by 0.2 kcal/mol), due to an endothermic heat (1.3 kcal/mol) and a water release of 8 mol H_2O/mol. The substitution of the UUU loop of *G2-UUU* with thymines (*G2-UUU* → *G2-TTT*) yielded similar thermodynamic contributions and a net release of 6 mol H_2O/mol. Therefore, these heat effects are associated with the hydration changes accompanied by the inclusion of the methyl groups.

Conclusions

We used a combination of spectroscopic and calorimetric techniques to investigate the unfolding thermodynamics of the K^+ form of ten G-quadruplexes, based on the sequence of the thrombin aptamer, with different loop sequences. All oligonucleotides form very stable intramolecular G-quadruplexes in the chair conformation. The favorable folding of each G-quadruplex results from the characteristic compensation of a favorable enthalpy and unfavorable entropy contributions, uptake of counterions and release of water molecules. The thermodynamic contributions of the loops were obtained by subtracting the thermodynamic contributions of a single G-quartet stack from each of the experimental thermodynamic profiles. This exercise indicates that the inclusion of loops to a G-quartet stack increases the overall stability of a G-quadruplex, due to favorable heat contributions, additional uptake of counterions and higher water releases. The thermodynamic contributions for specific base substitutions in the loops were also discussed. Relative to the control molecule (thrombin aptamer), every base substitution in the loops caused a decreased in the thermal stability of the G-quadruplex and a higher exothermic heat, which is explained in terms of stacked loops onto the G-quartets and base−base stacking within the loops, and their overall hydration contributions. In summary, changes in the sequence of the loops of G-quadruplexes can have a significant effect on their overall stability.

The present study is important because it provides a better understanding of how individual bases in the loops of G-quadruplexes may provide additional stability, and their effects on the magnitude of the thermodynamic forces (both enthalpic and entropic), ion, and water binding.

Acknowledgment. This work was supported by Grant MCB-0616005 from the National Science Foundation and a GAANN Fellowship to C.M.O.

References and Notes

(1) Folini, M.; Pennati, M.; Zaffaroni, N. *Curr. Med. Chem.−Anti Cancer Agents* **2002**, *5* (2), 605.
(2) Neidle, S.; Read, M. A. *Biopolym. Nucleic Acid Sci.* **2001**, *56*, 195.
(3) Huard, S.; Autexier, C. *Curr. Med. Chem.−Anti Cancer Agents* **2002**, *5*, 577.
(4) Mills, M.; Lacroix, L.; Arimondo, P. B.; Leroy, J. L.; Francois, J. C.; Klump, H.; Mergny, J. L. *Curr. Med. Chem.−Anti Cancer Agents* **2002**, *5*, 627.
(5) Kyo, S.; Inoue, M. *Curr. Med. Chem.−Anti Cancer Agents* **2002**, *5*, 613.
(6) DePamphilis, M. L. *Annu. Rev. Biochem.* **1993**, *62*, 29.
(7) Blackburn, E. H. *Nature* **1991**, *350*, 569.
(8) Sundquist, W. I.; Klug, A. *Nature* **1989**, *342*, 825.
(9) Williamson, J. R.; Raghuraman, M. K.; Cech, T. R. *Cell* **1989**, *59*, 871.
(10) Han, H.; Hurley, L. H. *Trends. Pharmacol. Sci.* **2000**, *21*, 136.
(11) Bock, L. C.; Griffin, L. C.; Latham, J. A.; Vermaas, E. H.; Toole, J. J. *Nature* **1992**, *355*, 564.
(12) Wang, K. Y.; Krawczyk, S. H.; Bischofberger, N.; Swaminathan, S.; Bolton, P. H. *Biochemistry* **1993**, *32*, 11285.
(13) Rando, R. F.; Ojwang, J.; Elbaggari, A.; Reyes, G. R.; Tinder, R.; McGrath, M. S.; Hogan, M. E. *J. Biol. Chem.* **1995**, *270*, 1754.

(14) Siebenlist, U.; Henninghausen, L.; Battey, J.; Leder, P. *Cell* **1984**, *37*, 381.
(15) Boles, T. C.; Hogan, M. E. *Biochemistry* **1987**, *26*, 367.
(16) Simonsson, T.; Pribylova, M.; Vorlickova, M. *Biochem. Biophys. Res. Commun.* **2000**, *278*, 158.
(17) Sakatsume, O.; Tsutsui, H.; Wang, Y.; Gao, H.; Tang, X.; Yamauchi, T.; Murata, T.; Itakura, K.; Yokoyama, K. K. *J. Biol. Chem.* **1996**, *271*, 31322.
(18) Postel, E. H.; Berberich, S. J.; Rooney, J. W.; Kaetzel, D. M. *J. Bioenerg. Biomembr.* **2000**, *32*, 277.
(19) Michelotti, E. F.; Tomonaga, T.; Krutzsch, H.; Levens, D. *J. Biol. Chem.* **1995**, *270*, 9494.
(20) Ji, L.; Arcinas, M.; Boxer, L. M. *J. Biol. Chem.* **1995**, *270*, 13392.
(21) Shafer, R. H.; Smirnov, I. *Biopolymers* **2001**, *56*, 209.
(22) Henderson, E.; Hardin, C. C.; Walk, S. K.; Tinoco Jr, I.; Blackburn, E. H. *Cell* **1987**, *51*, 899.
(23) Macaya, R. F.; Schultze, P.; Smith, F. W.; Roe, J. A.; Feigon, J. *Proc. Natl. Acad. Sci. U.S.A.* **1993**, *90*, 3745.
(24) Schultze, P.; Macaya, R. F.; Feigon, J. *J. Mol. Biol.* **1994**, *234*, 1532.
(25) Keniry, M. A.; Owne, E. A.; Shafer, R. H. *Nucleic Acids Res.* **1997**, *25*, 4389.
(26) Olsen, C. M.; Gmeiner, W. H.; Marky, L. A. *J. Phys. Chem. B* **2006**, *110*, 6962.
(27) Hazel, P.; Huppert, J.; Balasubramanian, S.; Neidle, S. *J. Am. Chem. Soc.* **2004**, *126*, 16405.
(28) Blackburn, E. H. *Cell* **1994**, *77*, 621.
(29) Sen, D.; Gilbert, W. *Biochemistry* **1992**, *31*, 65.
(30) Seenisamy, J.; Bashyam, S.; Gokhale, V.; Vankayalapati, H.; Sun, D.; Siddiqui-Jain, A.; Streiner, N.; Shin-ya, K.; White, E.; Wilson, W. D.; Hurley, L. H. *J. Am. Chem. Soc.* **2005**, *127*, 2944.
(31) Mills, M.; Lacroix, L.; Arimondo, P. B.; Leroy, J. L.; Francois, J. C.; Klump, H.; Mergny, J.-L. *Curr. Med. Chem.−Anti Cancer Agents* **2002**, *5*, 627.
(32) Siddiqui-Jain, A.; Grand, C. L.; Bearss, D. J.; Hurley, L. H. *Proc. Natl Acad. Sci. U.S.A.* **2002**, *99*, 11593.
(33) Duquette, M. L.; Handa, P.; Vincent, J. A.; Taylor, A. F.; Maizels, N. *Genes Dev.* **2004**, *18*, 1618.
(34) Sacca, B.; Lacroix, L.; Mergny, J.-L. *Nucleic Acids Res.* **2005**, *33*, 1182.
(35) Wang, Y.; Patel, D. J. *Structure* **1993**, *1*, 263.
(36) Parkinson, G. N.; Lee, M. P. H.; Neidle, S. *Nature* **2002**, *417*, 876.
(37) Schultze, P.; Hud, N. V.; Smith, F. W.; Feigon, J. *Nucleic Acids Res.* **1999**, *27*, 3018.
(38) Smith, W. F.; Feigon, J. *Biochemistry* **1993**, *32*, 8682.
(39) Tang, C.-F.; Shafer, R. H. *J. Am. Chem. Soc.* **2006**, *128*, 5966.
(40) Smirnov, I.; Schafer, R. H. *Biochemistry* **2000**, *39*, 1462.
(41) Kankia, B. I.; Marky, L. A. *J. Am. Chem. Soc.* **2001**, *123*, 10799.
(42) Cantor, C. R.; Warshow, M. M.; Shapiro, H. *Biopolymers* **1970**, *9*, 1059.
(43) Marky, L. A.; Blumenfeld, K. S.; Kozlowski, S.; Breslauer, K. J. *Biopolymers* **1983**, *2*, 1247.
(44) Marky, L. A.; Breslauer, K. J. *Biopolymers* **1987**, *26*, 1601.
(45) Privalov, P. L.; Potekhin, S. A. *Methods Enzymol.* **1986**, *131*, 4.
(46) Kaushik, M.; Suehl, N.; Marky, L. A. *Biophys. Chem.* **2006**, *126*, 154.
(47) Cantor, C. R.; Schimmel, P. R. *Biophysical Chemistry*; W. H. Freeman and Company: New York, 1980.
(48) Spink, C. H.; Chaires, J. B. *Biochemistry* **1999**, *38*, 496.
(49) Lu, M.; Guo, Q.; Kallenbach, N. R. *Biochemistry* **1993**, *32*, 598.
(50) Dapic, V.; Abdomerovic, V.; Marrington, R.; Peberdy, J.; Rodger, A.; Trent, J. O.; Bates, P. J. *Nucleic Acids Res.* **2003**, *31*, 2097.
(51) Rentzeperis, D.; Alessi, K.; Marky, L. A. *Nucleic Acids Res.* **1993**, *21*, 2683.
(52) Shikiya, R. Energetics, Ion and Water Binding in the Unfolding of DNA: Nearest-Neighbor Contributions and Incorporation of Bulges, Mismatches, Cation Chains, and Base-Triplet Stacks. Ph.D. Dissertation, University of Nebraksa Medical Center, Omaha, NE, 2005.
(53) Kumar, N.; Maiti, S. *Nucleic Acids Res.* **2005**, *33*, 6723.
(54) Krakauer, H. *Biopolymers* **1972**, *11*, 811.
(55) Kankia, B. I.; Marky, L. A. *J. Phys. Chem. B* **1999**, *103*, 8759.

JP806853N